

Coupling resistance between n-type surface accumulation layer and p-type bulk in InN:Mg thin films

Christophe A. Hurni, Soojeong Choi, Oliver Bierwagen, and James S. Speck

Citation: *Appl. Phys. Lett.* **100**, 082106 (2012); doi: 10.1063/1.3680102

View online: <http://dx.doi.org/10.1063/1.3680102>

View Table of Contents: <http://apl.aip.org/resource/1/APPLAB/v100/i8>

Published by the [American Institute of Physics](#).

Related Articles

Post growth annealing study on long wavelength infrared InAs/GaSb superlattices
J. Appl. Phys. **111**, 053113 (2012)

Bi-induced p-type conductivity in nominally undoped Ga(AsBi)
Appl. Phys. Lett. **100**, 092109 (2012)

Properties of In_xGa_{1-x}N films in terahertz range
Appl. Phys. Lett. **100**, 071913 (2012)

Characterization of thin-film GaAs diodes grown on germanium-on-insulator on Si substrate
J. Appl. Phys. **111**, 044504 (2012)

Well-to-well non-uniformity in InGaN/GaN multiple quantum wells characterized by capacitance-voltage measurement with additional laser illumination
Appl. Phys. Lett. **100**, 071910 (2012)

Additional information on *Appl. Phys. Lett.*

Journal Homepage: <http://apl.aip.org/>

Journal Information: http://apl.aip.org/about/about_the_journal

Top downloads: http://apl.aip.org/features/most_downloaded

Information for Authors: <http://apl.aip.org/authors>

ADVERTISEMENT

<p>INSTRUMENTS FOR ADVANCED SCIENCE</p> 	<p>Gas Analysis</p> <p>dynamic measurement of reaction gas streams catalysis and thermal analysis molecular beam studies dissolved species probes fermentation, environmental and ecological studies</p>	<p>Surface Science</p> <p>UHV TPD SIMS end point detection in ion beam etch elemental imaging - surface mapping</p>	<p>Plasma Diagnostics</p> <p>plasma source characterisation etch and deposition process reaction kinetic studies analysis of neutral and radical species</p>	<p>Vacuum Analysis</p> <p>partial pressure measurement and control of process gases reactive sputter process control vacuum diagnostics vacuum coating process monitoring</p>
	<p>contact Hiden Analytical for further details: info@hiden.co.uk www.HidenAnalytical.com CLICK TO VIEW OUR PRODUCT CATALOGUE</p>			

Coupling resistance between n-type surface accumulation layer and p-type bulk in InN:Mg thin films

Christophe A. Hurni,^{1,a)} Soojeong Choi,¹ Oliver Bierwagen,² and James S. Speck¹

¹Materials Department, University of California, Santa Barbara, 93106-5050 California, USA

²Paul-Drude-Institut für Festkörperelektronik, Hausvogteiplatz 5-7, D-10117 Berlin, Germany

(Received 5 December 2011; accepted 9 January 2012; published online 22 February 2012)

Indium nitride is the least studied of the III-nitride though it has great potential due to its small bandgap of 0.65 eV and a small effective electron mass. InN:Mg was recently confirmed to be p-type. However, Hall measurements on InN:Mg still show n-type conductivity, even when InN:Mg is very thick. Some studies have suggested the possibility of a high coupling resistance between the surface electron accumulation and the bulk p-InN. In this study, we show through vertical and transmission-line model measurement that this coupling resistance is small and should not affect conductivity and Hall measurements. © 2012 American Institute of Physics. [doi:10.1063/1.3680102]

Gallium nitride (GaN) and indium gallium nitride (InGaN) are widely studied because of their opto-electronic applications. In-rich InGaN or indium nitride (InN) have been less studied despite very attractive properties, including a very small bandgap, which is promising for infrared applications and a small electron effective mass, which is attractive for high-speed transistors.¹ InN has a very high electron affinity which creates a surface electron accumulation layer (SEAL).² The presence of the SEAL makes electrical measurement of bulk InN challenging. In particular, InN:Mg, which has been shown to be p-type by electrolyte-based capacitance-voltage measurements³ and thermopower measurements,⁴ only shows n-type conductivity in Hall measurements. The electrical behavior of the internal p-n junction, made of the n-type SEAL and the p-type bulk InN:Mg is poorly understood. Some recent articles have suggested that this junction has a high series resistance, which may prevent the observation of holes in Hall measurement, even with thick InN:Mg samples.^{5,6}

In this article, we investigate the rectifying behavior of this junction as well as its resistance. We show that etched mesas also exhibit highly conductive pathways along the side walls or due to current crowding at the side walls, and that vertical measurements of the internal p-n junction is not possible with a vertical junction process. Using the alternative approach of transmission-line model (TLM) measurements and modeling, we show that this junction is not rectifying and can be modeled with small resistance.

For this study, different thicknesses InN:Mg were grown by plasma assisted molecular beam epitaxy on semi-insulating GaN:Fe substrates grown by metal organic chemical vapor deposition by Lumilog. All the samples include a 100 nm GaN:C layer under the InN:Mg layer to improve isolation. The Mg concentration was around $1.6 \times 10^{19} \text{ cm}^{-3}$. More details about the growth and the samples is reported elsewhere.⁷

To investigate a p-n junction, it is natural to consider vertical measurements, with etched mesas, if the sidewalls

do not dominate the transport.⁹ To assess if vertical etched surface were conductive, mesas of different sizes and aspect ratios were etched by standard BCl_3/Cl_2 reactive ion etching (RIE) on a $2.4 \mu\text{m}$ -thick InN:Mg sample. The depth of the mesa etching was 250 nm. It was observed that GaN would etch about five times faster in the same RIE conditions. Ti/Au (30 nm/300 nm) metal contact were then deposited by electron-beam evaporation on the top of the mesa and around the mesa. The process is similar to a diode process, with the same metal for the top and the bottom contact.

The top left inset on Figure 1 shows the mask that was used. The mesa sizes ranged from $100 \times 100 \mu\text{m}^2$ to $500 \times 500 \mu\text{m}^2$. For areas from $200 \times 200 \mu\text{m}^2$ to $500 \times 500 \mu\text{m}^2$, there were diodes with three different shapes: a standard square mesa with a full bottom contact (S-diode), a square mesa with a half bottom contact (L-diode), and a mesa with fingers (F-diode). The different areas and perimeters are given in Table I.

Figure 1 shows the current voltage (I-V) characteristics of the diodes with an area of $400 \times 400 \mu\text{m}^2$. It can be seen that the I-V characteristics are very linear so that if current is going through the junction, there is no rectifying behavior.

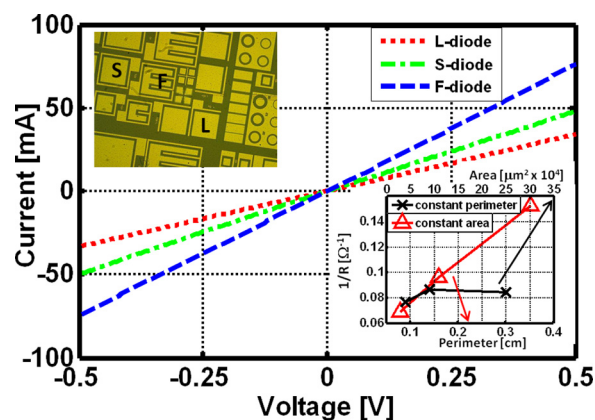


FIG. 1. (Color online) Top left: microscope image of the mask after processing. Bottom right: conductance in function of perimeter for $16 \times 10^4 \mu\text{m}^2$ diodes and conductance for the diodes with perimeter of 1000, 1100 and 1200 μm . Main: I-V characteristics of $16 \times 10^4 \mu\text{m}^2$ diodes.

^{a)}Electronic mail: hurni@engr.ucsb.edu.

TABLE I. Area and perimeter of the diodes.

Area [$\mu\text{m}^2 \times 10^4$]	Perimeter [μm]		
	L-diode	S-diode	F-diode
1	—	400	—
4	400	800	1100
9	600	1200	2290
16	800	1600	3530
25	1000	2000	5570

The bottom right inset of Figure 1 shows the conductance $1/R$ in function of perimeter for the diodes with constant area $400 \times 400 \mu\text{m}^2$ as well as the conductance for the diodes with similar perimeter (1000, 1100, 1200 μm) but different areas. There is a clear linear dependence of the conductance on perimeter length, which indicates a conductance limited by lateral rather than vertical transport. The conductance does not seem to scale with area. For mesas with the same area, one can assume that $\sigma = 1/R = a \cdot p + b$, with p the perimeter, a and b constants. If the distance between the contacts is $L = 20.25 \mu\text{m}$, which is the lateral spacing of $20 \mu\text{m}$, with the $0.25 \mu\text{m}$ vertical etch, then $R_a = \frac{1}{L \cdot a}$, with R_a the sheet resistance that is surface related. The extracted value for R_a ranges from 1000 to 2100 Ω/\square , which is similar to the SEAL sheet resistance measured with low temperature Hall measurements on the same samples using pressed down In contacts.^{6,8} The sample was processed again with a 750 nm mesa etch and a third time with a 1500 nm depth. Every etch depth yielded similar results for the sheet resistance R_a . Unfortunately the lateral distances will always be larger than the vertical distances, which prevents a precise measurement of the sheet resistance of the etched surfaces. However this shows that they are conductive, and have a resistance on the same order of magnitude than the SEAL.

The vertical transport of the mesa could be due to conduction along a SEAL of the etched mesa sidewalls, or conduction through the SEAL-p-bulk-SEAL interfaces with current crowding at the edge of the mesas and contacts. Current crowding is likely as the resistivity of the SEAL is smaller than that of the InN:Mg. With the present experiments, however, we cannot distinguish both cases but conduction along the non-polar sidewalls is likely present as non-polar surfaces have been shown to be conductive.¹⁰

Since vertical measurements could not yield the coupling resistance between the SEAL and the bulk InN:Mg, the second set of experiments involved lateral TLM measurements. A $0.4 \mu\text{m}$ thick InN:Mg sample was used for this process. The mesas were etched using RIE with BCl_3/Cl_2 . The etch was $0.45 \mu\text{m}$, down to the insulating GaN:C for mesa isolation. The Ti/Au (30 nm/300 nm) contacts were deposited by electron-beam evaporation. The TLM width was $100 \mu\text{m}$ and the spacings were 5, 10, 15, 20, 25, and $30 \mu\text{m}$. The mask also included Van der Pauw Hall patterns. The Hall measurements with these patterns resulted in an apparent n-type sheet concentration of $7.5 \times 10^{13} \text{cm}^{-2}$ and an apparent sheet resistance of $1130 \Omega/\square$. The standard one layer TLM analysis yielded the same apparent sheet resistance as the Van de Pauw measurement, and an apparent specific contact resistance of $2\text{-}3 \times 10^{-4} \Omega \text{cm}^2$. These values are consistent

with the room temperature (RT) Hall measurements done with pressed down In contacts on the same sample.^{6,8}

Figure 2 shows the measured resistance R_{TLM} for each spacing. The good linearity of the I-V curves (shown at the bottom right of Figure 2) implies again no rectifying behavior of the internal p-n junction. Therefore, from here on, the internal p-n junction will be considered to behave like a linear resistor, modeled by a coupling resistance, with the unit of a contact resistance.

The results were analyzed within the two-layer TLM model developed by Look,¹¹ with the main equations shown below

$$R = 2C_1 C_2 \left(\frac{R_{S1}}{wk_1} \right) + C_3 \left(\frac{R_{S1} l}{w} \right), \text{ with} \quad (1)$$

$$C_1 = 1 + \frac{R_{S1}}{R_{S2}} \frac{1}{1 + k_1/k_2},$$

$$C_2 = \frac{1 + \left(\frac{1}{(1+R_{S2}/R_{S1})} \right) \left[\frac{k_1}{k} + \frac{k_2}{k} \left(\frac{1}{(1+k_1/k_2)} + \frac{R_{S2}}{R_{S1}} \right) \right] F(kl)}{1 + \left[\frac{k_2}{k} \left(1 + \frac{R_{S2}}{R_{S1}} \right) / \left(1 + \frac{R_{S1}/R_{S2}}{1+k_1/k_2} \right) \right] F(kl)},$$

$$C_3 = \frac{R_{S2}}{R_{S1} + R_{S2}}, \quad F(kl) = \frac{\sinh(kl)}{1 + \cosh(kl)},$$

$$k^2 = \frac{R_{S1} + R_{S2}}{\rho_{C2}}, \quad k_1^2 = \frac{R_{S1}}{\rho_{C1}}, \quad k_2^2 = \frac{R_{S2}}{\rho_{C2}}.$$

R is the resistance for any spacing l and width w . The contact resistance of the top metal contact to the SEAL is called ρ_{C1} and the coupling resistance between the SEAL and the InN:Mg is ρ_{C2} , which have the units of a contact resistance. The sheet resistance of the SEAL is R_{S1} and the sheet resistance of the bulk In:Mg is R_{S2} , as shown in the inset of Figure 2. Unlike in Look's original model, we assumed that the sheet resistance under and between the contacts was the same, which is very reasonable, since the contacts were not annealed. Look's equations are only valid under the assumption that $\rho_2 \gg \rho_1$.

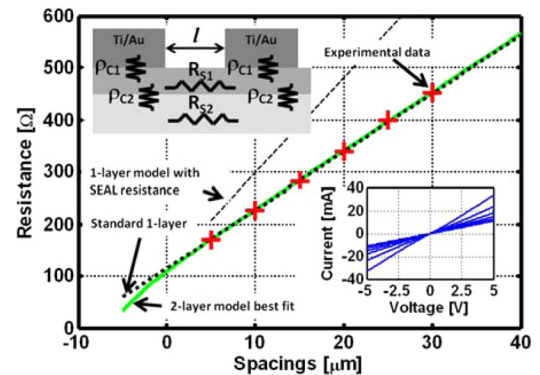


FIG. 2. (Color online) Top left: resistances in the Look's bi-layer model. Bottom right: I-V curves for $5 \mu\text{m}$ to $30 \mu\text{m}$ spacings. Main: measured TLM resistances R_{TLM} in function of spacing, with standard 1-layer linear extrapolation yielding an apparent sheet concentration of $1130 \Omega/\square$ and an apparent specific contact resistance of $2\text{-}3 \times 10^{-4} \Omega \text{cm}^2$ and best fit with a 2-layer TLM model, with $R_{S1} = 1830 \Omega/\square$, $R_{S2} = 2900 \Omega/\square$, $\rho_{C1} = 1.1 \times 10^{-4} \Omega \text{cm}^2$ and $\rho_{C2} = 7 \times 10^{-4} \Omega \text{cm}^2$. The thin dotted line is the expected TLM resistance if current was only going through the SEAL, assuming $R_{S1} = 1830 \Omega/\square$.

Since the model is using four parameters, a unique solution is unlikely to be found through a least-square fit, with only six data points. Therefore, we are limiting as many parameters as possible by using the results of other transport measurements on the same sample series.

One parameter that can be extracted without relying on the coupling resistance in question ρ_{C2} is the SEAL sheet resistance R_{S1} . Mayer *et al.*⁶ showed that upon cooling from RT to 100 K, the apparent sheet resistance of the InN:Mg samples of different thicknesses was strongly increasing due to carrier freeze-out in the bulk InN:Mg. Below 100 K the apparent sheet resistance did not depend on the thickness anymore, and only the sheet resistance R_{S1} of the SEAL is measured. However, the sheet resistance of the SEAL was still temperature dependent below 100 K, which suggests that the SEAL is not fully degenerate.⁸ Hence one cannot simply measure the SEAL sheet resistance at low temperature and assume that it is the same at RT. Instead, we estimate the SEAL sheet resistance R_{S1} at RT by extrapolating the low temperature sheet resistance based on the relative change of a 50 nm InN:Mg sample which had almost negligible p-type contribution to the sheet resistance, as shown on Figure 3. This estimation does not rely on any assumption on the coupling resistance, since InN:Mg bulk is assumed to be not conductive at low temperature. Bierwagen *et al.*⁸ goes further and estimates the resistivity of the bulk InN:Mg assuming a low coupling resistance, but this result was not used here. This estimation for the sheet resistance R_{S1} of the SEAL was $1830 \pm 100 \Omega/\square$ at RT.

The fact that the apparent sheet resistance extracted by the single-layer model differs significantly from R_{S1} implies that current is also flowing through the bulk InN:Mg. This is shown in Figure 2, which shows the 1-layer TLM resistance that one would expect with $R_{S1} \sim 1830 \Omega/\square$. The apparent specific contact resistance of $3 \times 10^{-4} \Omega \text{ cm}^2$ extracted from the 1-layer model was used as a higher limit for ρ_{C1} , as the apparent specific contact resistance accounts for both ρ_{C1}

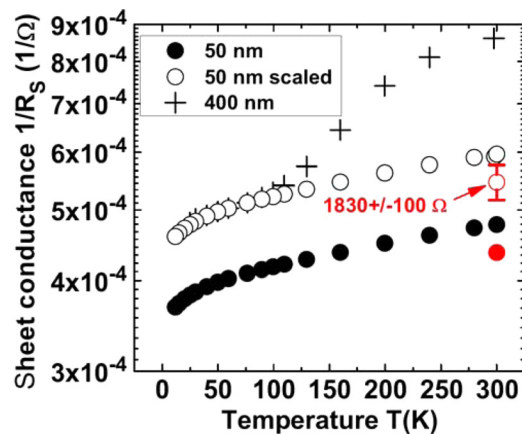


FIG. 3. (Color online) Sheet conductance of a 400 nm and a 50 nm thick InN:Mg film as function of temperature. The open symbols are the estimated sheet conductance of the SEAL of the 400 nm InN:Mg sample in function of temperature, assuming the same relative temperature dependence than the 50 nm InN:Mg sample. For this estimation the low temperature (when only the SEAL is conductive) conductance of the 50 nm InN:Mg sample was scaled to that of the 400 nm film. The contribution of the bulk for the 50 nm InN:Mg sample (estimated in Ref. 8) is corrected for in the vertically-offset data points but has only a minor influence.

and ρ_{C2} . The specific contact resistance of a 10 nm unintentionally doped (UID) InN grown around the same time and processed the same way, was found to be $1 \times 10^{-5} \Omega \text{ cm}^2$ and this was used as a lower limit for ρ_{C1} .

Look notes that after a coupling distance, the bi-layer structure can be considered as parallel resistor, and the resistance as function of distance will be linear. In our case, since the measured TLM resistances R_{TLM} are linear in function of spacing, this distance has to be on the order of the shortest spacing or shorter. This means that $k^{-1} = \sqrt{\frac{\rho_{C2}}{R_{S1} + R_{S2}}} \leq 5 \mu\text{m}$.

With these strong boundaries and conditions, we applied a least square fit regression to the data, despite the limited data points, finding a minimum for the error $= ||R - R_{TLM}||$. R was calculated with Eq. (1). The values for the best fits are given in Table II, and the best fit for $R_{S1} = 1830 \Omega/\square$ is plotted in Figure 2. It should be pointed out that the extracted value for ρ_{C2} is a higher limit, imposed by the condition $\rho_{C2} \gg \rho_{C1}$ of Look's original model. In the least-square fit, we imposed $\rho_{C2} > 6 \cdot \rho_{C1}$ and it can be seen that the values of ρ_{C2} are close to the minimum value imposed by the least-square fit. The actual value of ρ_{C2} could therefore be smaller, in which case, the assumptions made in Look's model would not be valid and a simple parallel resistor case where both layers are fully connected would be more appropriate. In all the cases, the condition $k^{-1} = \sqrt{\frac{\rho_{C2}}{R_{S1} + R_{S2}}} \leq 5 \mu\text{m}$ is respected, which implies good coupling. Also, it can be checked that in all cases, the equivalent parallel sheet resistance, assuming good coupling $\frac{R_{S1} \cdot R_{S2}}{R_{S1} + R_{S2}} \sim 1130 \Omega/\square$, which is the apparent sheet resistance from the 1-layer TLM.

The low extracted value for ρ_{C2} suggests that the p-n junction formed by the SEAL and the InN:Mg may act like a tunnel junction. This is reasonable since InN has a small bandgap and the doping on both sides is high. With the doping in our sample, the depletion should be under 10 nm, assuming published constants,¹ like in tunnel diodes. Also, the highly dislocated InN grown under In rich conditions is likely to create leakage paths and could be the reason for the non rectifying behavior of the junction.¹²

In many studies about InN:Mg, the samples are unprocessed and the contacts are made of pressed down indium pieces that are far apart. If one assumes a contact width of $w = 1 \text{ mm}$ and a distance of $l = 10 \text{ mm}$ between the contacts, the total resistance of such a sample assuming parallel conductors perfectly connected is $\frac{l}{w} \cdot \frac{R_{S1} \cdot R_{S2}}{R_{S1} + R_{S2}} \cdot l \sim 11300 \Omega$. The calculation of R from Eq. (1) with our best fit parameters in these conditions showed that the contribution of the contact and coupling resistances will be about 20Ω , which is not significant.

In summary, vertical transport measurements with etched mesas normal to the In-face of InN have shown no sign of rectification, and a high conductivity due to surface

TABLE II. Best least square fit of equation (1) to the data R_{TLM} .

R_{S1} [Ω/\square]	R_{S2} [Ω/\square]	ρ_{C1} [$\Omega \text{ cm}^2$]	ρ_{C2} [$\Omega \text{ cm}^2$]
1730	3300	1.2×10^{-4}	8×10^{-4}
1830	2900	1.1×10^{-4}	7×10^{-4}
1930	2700	1×10^{-4}	6×10^{-4}

conduction on the side walls or current crowding at the side walls. Lateral transport measurements analyzed with the dual-layer TLM model indicated that the junction between n-type SEAL and the p-type bulk InN:Mg is not rectifying, and has a junction resistance as low as $6\text{--}8 \times 10^{-4} \Omega \text{ cm}^2$ or lower. This junction resistance should not play a role for conductivity and Hall measurements when contacts are far away, like it is often the case in unprocessed samples with pressed down In contacts.

The authors thank M. A. Mayer, W. Waluckiewicz, and D. Look for fruitful discussions. This work was supported by AFOSR, with K. Reinhardt and J. Hwang as program managers.

¹J. Wu, *J. Appl. Phys.* **106**(1), 011101 (2009).

²I. Mahboob, T.D. Veal, C.F. McConville, H. Lu, and W.J. Schaff, *Phys. Rev. Lett.* **92**, 3 (2004).

³R. E. Jones, K. M. Yu, S. X. Li, W. Walukiewicz, J. W. Ager, E. E. Haller, H. Lu, and W. J. Schaff, *Phys. Rev. Lett.* **96**, 125505 (2004).

⁴J. W. Ager, N. Miller, R. E. Jones, K. M. Yu, J. Wu, W. J. Schaff, and W. Walukiewicz, *Physica Status Solidi (b)* **245**, 873 (2008).

⁵E. Alarcon-Llado, M. A. Mayer, B. W. Boudouris, R. A. Segalman, N. Miller, T. Yamaguchi, K. Wang, Y. Nanishi, E. E. Haller, and J. W. Ager, *Appl. Phys. Lett.* **99**(10), 102106 (2011).

⁶M. A. Mayer, S. Choi, O. Bierwagen, H. M. Smith, E. E. Haller, J. S. Speck, W. Walukiewicz, *J. Appl. Phys.* **110**, 123707 (2011).

⁷S. Choi and J. S. Speck, "Magnesium doped and unintentionally doped indium nitride grown by plasma assisted molecular beam epitaxy method" (unpublished).

⁸O. Bierwagen, S. Choi, and J. S. Speck, "Hall and Seebeck measurement of a p-n layer stack: Determining InN bulk hole transport properties in the presence of a strong surface electron accumulation layer," *Phys. Rev.* (submitted).

⁹C. A. Hurni, O. Bierwagen, J. R. Lang, B. M. McSkimming, C. S. Gallinat, E. C. Young, D. A. Browne, U. K. Mishra, and J. S. Speck, *Appl. Phys. Lett.* **97**(22), 222113 (2011).

¹⁰W. M. Linhart, T. D. Veal, P. D. C. King, G. Koblmüller, C. S. Gallinat, J. S. Speck, and C. F. McConville, *Appl. Phys. Lett.* **97**, 112103 (2010).

¹¹D. C. Look, *IEEE Trans. Electron Devices* **35**(2) 133 (1988).

¹²S. W. Kaun, M. H. Wong, S. Dasgupta, S. Choi, R. Choi, U. K. Mishra, and J. S. Speck, *Appl. Phys. Express* **4**, 024101 (2011).